



HAL
open science

Observations of the seasonality of the Antarctic microseismic signal, and its association to sea ice variability

Mélanie Grob, Alessia Maggi, Eléonore Stutzmann

► **To cite this version:**

Mélanie Grob, Alessia Maggi, Eléonore Stutzmann. Observations of the seasonality of the Antarctic
microseismic signal, and its association to sea ice variability. *Geophysical Research Letters*, 2011, 38,
pp.L11302. 10.1029/2011GL047525 . hal-00679388

HAL Id: hal-00679388

<https://hal.science/hal-00679388>

Submitted on 15 Mar 2012

HAL is a multi-disciplinary open access archive for the deposit and dissemination of scientific research documents, whether they are published or not. The documents may come from teaching and research institutions in France or abroad, or from public or private research centers.

L'archive ouverte pluridisciplinaire **HAL**, est destinée au dépôt et à la diffusion de documents scientifiques de niveau recherche, publiés ou non, émanant des établissements d'enseignement et de recherche français ou étrangers, des laboratoires publics ou privés.

Observations of the seasonality of the Antarctic microseismic signal, and its association to sea ice variability

M. Grob,^{1,3} A. Maggi,¹ and E. Stutzmann,²

¹Institut de Physique du Globe de
Strasbourg, Université de
Strasbourg/EOST, CNRS, 5 rue René
Descartes, 67084 Strasbourg Cedex, France.

²Institut de Physique du Globe de Paris
Paris Sorbonne Cité CNRS UMR 7154, 1
rue Jussieu, 75005 Paris, France.

³now at Department of Physics,
University of Alberta, 11322 - 89 Avenue,
Edmonton AB T6G 2G7, Canada.

(grob@ualberta.ca)

Seismic noise spectra at all seismic stations display two peaks in the 1-20 s period band, called primary and secondary microseisms. They are caused by the coupling of ocean waves into Rayleigh waves. At most locations, microseismic power is greater during local winter (when nearby oceans are stormier) than local summer. This tendency is reversed for stations in Antarctica, where growth of local winter sea ice seems to impede microseism generation in near coastal areas. A decade of continuous data from coastal seismic stations in Antarctica show systematic seasonality in microseismic signal levels, and demonstrate associations with both broad-scale and local sea-ice conditions. Primary microseisms are known to be generated at the coast and the modulation that we observe can be associated with sea-ice variations both in the vicinity of the station and along other Antarctic coasts. The similar modulation of short-period secondary microseisms corroborates their mostly near-coastal origin, while the continued presence of long-period secondary microseisms suggests more distant source regions. These observations could be used to extend the monitoring of climate variability prior to the availability of satellite-derived climate indicators.

1. Introduction

Analyses of seismic noise spectra ubiquitously show broad energetic peaks over a 3-20 s period band, primarily composed of Rayleigh waves, and commonly referred to as primary (10-20 s) and secondary (3-10 s) microseisms. These microseisms are due to ocean gravity wave interactions that cause pressure oscillations, which in turn generate seismic waves at the ocean floor [Longuet-Higgins, 1950; Tanimoto, 2007; Kedar *et al.*, 2008]. Primary microseisms are generated when ocean gravity waves reach shallow water near the coast and interact with the sloping seafloor, either by breaking or shoaling [Hasselmann, 1963]. These seismic waves have periods similar to the incident ocean gravity waves. Secondary microseisms are more energetic, and are generated by standing or colliding waves within the ocean wave field near the coast or in the deep ocean [e.g. Haubrich and Mc Camy, 1969; Friedrich *et al.*, 1998; Chevrot *et al.*, 2007; Bromirski *et al.*, 1999]. These in turn create standing pressure fluctuations at the ocean bottom at half the period of the ocean waves. The variations in microseismic power have been linked to the presence of ocean storms [Bromirski and Duennebier, 2002; Barruol *et al.*, 2006; Gerstoft and Tanimoto, 2007; Aster *et al.*, 2008, 2010].

Stutzmann et al. [2009] analyse seismic noise spectra at all stations of the global GEOSCOPE network, and show that microseismic power is greater during local winter at the high latitudes of both hemispheres. This seasonality is explained by the seasonal increase of nearby oceanic storms. The only GEOSCOPE station that displays a different behaviour is Dumont d'Urville (DRV) in Antarctica, where microseismic amplitude is weaker in winter than in summer. *Stutzmann et al.* [2009] link this phenomenon to the

presence of sea ice-floe, which prevents incoming swells from reaching the coast, thereby impeding both direct coupling at the coast (responsible for the primary microseisms) and swell reflection (responsible for the secondary microseisms). In this study, we extend the analysis to seismic stations at other coastal regions of Antarctica, in order to validate the observations made at DRV.

Sea-ice extension and concentration vary seasonally (following the cycle of ice-floe formation and dislocation) and inter-annually [*Cavalieri and Parkinson, 2008*]. They are important factors for modelling climate variability, as they influence the energy exchange between ocean and atmosphere. Sea ice has been continuously monitored by satellite since 1979, using passive microwave radiometers. We take advantage of this extensive data-set to investigate in greater detail the correlation between microseism power and ice-floe presence, and briefly discuss the use of this seismic observation for investigating climate variations.

2. Microseism analysis

We analyze microseismic signals over the time period 2000-2009 for ten stations located on or near the coast of Antarctica: SNAA.GE, SYO.PS, MAW.AU, CASY.IU, DRV.G, VNDA.GT, SBA.IU, LONW.YT, SIPL.YT, PMSA.IU. The data are available from IRIS (Incorporated Research Institutions for Seismology) DMC for most stations, and directly from the station operator for SYO (2005-2009).

We calculate robust power spectral densities (PSD) of waveform data from continuous, vertical component seismic recordings, using the *Chave et al. [1987]* method. Specifically, we remove the instrument response, and segment the waveforms into hour long time

windows that overlap by 50%. Earthquakes and glitches are eliminated by using an iterative algorithm, and we calculate a smoothed Fourier transform for each data segment. The energy spectrum is computed using the median over all windows, and is averaged over 24 hours.

Figure 1a shows a typical microseism spectrogram over a year for CASY station. The primary microseism energy drops below -150 dB towards day 140 (end of May) and starts to rise again towards day 310 (November), though it does not reach the same level as during the beginning of the year. The secondary microseism energy also drops near the end of May and, like the primary microseism, begins to increase in November. The quiet period between May and November occurs during the austral winter, when sea-ice is most prevalent; the stronger microseismic signals at the beginning of the year occur when the coast is ice-free; the strengthening of the microseisms at year end occurs when ice concentration starts decreasing.

Decreasing microseism levels are observed at all coastal stations during the austral winter, although there are local variations in average energies and in the duration of the quiet period (Figure 1b). Average microseism energies are generally comparable between stations. Inland stations have lower energies due to their greater distance from the microseism source regions. An exception to this trend is MAW, which displays exceptionally low spectral amplitudes at all periods, possibly due to an incorrect instrument response. The strongest microseismic signals and the shortest quiet periods are observed at the most-northern station PMSA, located on the Antarctic peninsula, which is rarely iced-in and therefore more often exposed to ocean swells.

The winter-time microseismic attenuation repeats annually, with minor inter-annual variations. Figure 2 shows the annual microseismic spectra for SYO from 2001 to 2009, and clearly illustrates the first-order seasonality in both ice-cover and microseism energy. Lutzow-Holm Bay, near SYO, is ice-bound even in summer, which may explain the lower summer primary microseism energy at SYO compared to other coastal stations (e.g. CASY and DRV, see Figure 1b). There is some inter-annual variability in the level of microseism energy and the duration of the quiet periods at SYO, which can be related to localized inter-annual variations in ice-concentration. For example, the ~ 10 dB reduction in summer microseismic energy at SYO during 2005, 2007 and 2008 seems to be related to residual sea ice along the coast of Enderby land (see highlighted regions in Figure 2).

The seismic frequency of the microseismic peaks varies over time. Figure 3 contains 1-day spectra for SYO and CASY taken every 40 days throughout 2007, and shows that this variation is more pronounced for the secondary microseism, which is sensitive to specific coastal and/or wave-conditions that affect the generation of opposing waves [*Aster et al.*, 2010]. The primary microseism, generated by the direct interaction between incoming swell with the sloping seafloor, displays more consistent peak frequencies, which are systematically more stable and lower in winter than in summer (blue vs red highlighted regions in Figure 3). This shift towards longer periods during winter is likely to be related to the larger winter storms that produce longer gravity waves [*Webb*, 1998; *Stutzmann et al.*, 2000]. In winter, the seafloor interaction predominantly occurs farther from the Antarctic coast as the nearby regions are ice-covered. Therefore, the primary microseism

Rayleigh waves detected propagate longer distances to reach the stations, resulting in attenuation of a greater part of their shorter-period energy.

3. Sea ice observations

In Figures 1 and 2, we have reproduced average monthly ice concentration images from the National Snow and Ice Data Center (NSIDC) Sea Ice Index [*Fetterer et al.*, 2002]. Ice concentration, i.e. the fraction, or percentage, of ocean area covered by sea ice, is estimated by exploiting the differing passive microwave signatures of water and sea-ice: water has a highly polarized signature, while sea ice does not. The spatial resolution of sea-ice concentration estimates is 25 km. Detailed information about the satellites used, and the processing applied to obtain the Sea Ice Index images, is available from the NSIDC (<http://nsidc.org/data/g02135.html>).

In order to investigate the link between microseism power and ice coverage at temporal resolutions finer than one month, we also exploit daily gridded sea-ice concentrations from another NSIDC data product [*Cavalieri et al.*, 1996] that provides a consistent time series of sea ice concentrations at a grid cell size of 25×25 km, spanning the coverage of several microwave instruments. The raw satellite data are processed using the NASA Team algorithm developed by the Oceans and Ice Branch of the Laboratory of Hydrophseric Processes at NASA Goddard Space Flight Center (GSFC). More detailed information is available from NSIDC (<http://nsidc.org/data/nsidc-0051.html>). For each coastal seismic station, we extract daily average values of sea-ice concentration over a ~ 25 km-wide beam trending approximately normal to the closest coastline, and interpolate at regularly spaced distances from the coast in order to obtain average daily ice-concentration profiles. These

profiles are plotted alongside our microseism power plots for stations SYO, DRV, SBA and PMSA in Figure 4.

At all stations, the presence of sea-ice is clearly correlated with a decrease in microseismic power. This correlation is most clear at SYO, at which both primary and secondary microseism power decrease sharply when ice concentration reaches 80% at approximately 100 km (extent of the continental shelf) and 200 km from the coast respectively. The longer period primary and secondary microseisms persist for more extended time periods. Two instances of anomalously high austral winter secondary microseisms at SYO occur at the same time as localized instances of ice-breakup (black arrows in Figure 4). At DRV, the shortest period secondary microseisms (periods of 1-2 seconds, white bar) are no longer detected as soon as the bay ices-up, corroborating the *Stutzmann et al.* [2009] interpretation that they are probably due to local break-up of the nearby Astrolabe glacier. The broad-band primary microseisms (Figure 4a, black bar) persist 1-2 months after the local bay ices-up and the sea ice extends beyond the continental shelf and do not seem to correlate with local coastal conditions or the position of the local continental shelf. They may be generated by ice-free coastal regions elsewhere in Antarctica. The longest period primary and secondary microseisms remain detectable throughout the austral winter. At SBA, detection of shorter period secondary microseisms (Figure 4a, white bars) terminates as soon as Ross Bay is iced in, suggesting a local, possibly glacier related, microseism source. The longer period secondary microseisms continue throughout the winter, like at DRV, although with a broader frequency range. Near SBA, in contrast to the other stations, winter-time ice concentration is weaker close to the coast than at

greater distances. It is unclear how this could be related to the winter time microseismic noise. PMSA, being located on the Antarctic peninsula, is ice-free for most of the year, and has particularly strong microseisms. Two episodes of low levels of both primary and shorter-period secondary microseism energy at PMSA correspond to local increases in ice-concentration (Figure 4, black symbols).

4. Discussion

Antarctica is a perfect natural laboratory for gaining insights into the mechanisms of microseismic signal generation: the continent is surrounded by an often-stormy ocean, whose gravity wave interaction with its coasts is modulated by the presence or absence of sea-ice. Seismometer deployments directly on the Ross Ice Shelf have measured an annual attenuation by a factor of 100 of its swell-induced motion (7-40s period) at maximum ice extent [Cathles *et al.*, 2009]. The absence of swell in shallow water surrounding the continent during the austral winter impedes the formation of local primary microseisms; furthermore, the absence of free coasts during the same period impedes the formation of reflected swell wave-trains that contribute to the generation of near-coastal, high-frequency secondary microseisms.

During the austral summer, the broad frequency band over which we have observed primary microseisms is indicative of local coastal generation by well-dispersed oceanic swells from distant storms [e.g. Bromirski and Gerstoft, 2009]. The persistence of the long-period component of these primary microseisms during the austral winter is indicative of generation in more distant source regions (possible candidates are the coastal regions of

the Antarctic peninsula, South America, South Africa, southern Australia, Tasmania or New Zealand).

Longuet-Higgins [1950] showed that the largest amplitude secondary microseisms may be due to wave-wave interference in the mid ocean, although coastal reflexion may be a more common cause of microseisms of smaller amplitude. Since then, there have been many observations of both coastal sources [e.g. *Haubrich and Mc Camy*, 1969; *Friedrich et al.*, 1998; *Chevrot et al.*, 2007; *Bromirski et al.*, 1999; *Bromirski and Duennebier*, 2002], and offshore sources, the latter principally in the North Atlantic Ocean [*Stehly et al.*, 2006; *Kedar et al.*, 2008] and the Mediterranean sea [*Chevrot et al.*, 2007]. As Antarctic stations are close to the coast, we expect the secondary microseisms generated by local coastal sources to be amplified compared to those generated by more distant sources, since they are less attenuated due to their short propagation paths. This expectation is consistent with the observed correlation between ice cover and secondary microseism amplitude, which is particularly visible at short periods.

The persistence of the long-period secondary microseisms we have observed during the austral winter is indicative of one or more source regions at considerable distance from the Antarctic coast. A possible non-coastal source region could be the Kerguelen plateau, whose water-depth ($< 2000\text{m}$) is similar to that of the broad region south of Iceland identified by *Kedar et al.* [2008] as an off-shore source of secondary microseisms. Systematic identification of the source regions of the austral-winter microseisms, which is beyond the scope of this paper, would give valuable insights into the relative importance of coastal and pelagic microseism sources.

5. Conclusions

To first order, we have found that microseism power is anti-correlated with near-coastal ice presence, which opens the possibility of exploiting long-period seismic data to extend estimates of average ice-duration prior to the start of satellite measurements. The use of microseismic signal analysis for climate related inferences has been suggested by *Bromirski et al.* [1999]; *Aster et al.* [2008]; *Stutzmann et al.* [2009] for ice-free global seismic stations, by *Barruol et al.* [2006] for stations in French Polynesia, and by *Kedar et al.* [2008] for stations within the Labrador sea, for which the authors found that the microseisms were particularly sensitive to the exact position of the sea-ice boundary. It may be possible to extend microseismic studies in Antarctica back to the early to mid-1960s, at least for stations with a long history of recording such as DRV, which would, if successful, add one to two decades to the current, satellite-derived trends in climate indicators.

To second order, we have observed that variations in microseism power seem to be dependent on recurring local conditions, as shown from variable summer microseism levels at SYO and residual ice on the Enderby coast. More detailed study of such dependencies, including forward modeling of the microseismic signal from known wave and ice conditions, will be a great asset to understanding the regional scale variability associated with microseismic generation.

In conclusion, we have presented systematic observations of seasonality in microseismic signals from coastal stations in Antarctica, and have identified associations with both broad-scale and local sea-ice conditions. Further studies will be required to exploit these

observations fully in order to make robust inferences on the detailed mechanisms of microseismic signal generation, and possibly also on trends in climate indicators.

Acknowledgments. The authors would like to thank Lise Retailleau and Simon Boyat for processing part of the seismic data during their Master training. The facilities of the IRIS Data Management System, and specifically the IRIS Data Management Center, were used for access to waveform, metadata or products required in this study. The IRIS DMS is funded through the National Science Foundation and specifically the GEO Directorate through the Instrumentation and Facilities Program of the National Science Foundation under Cooperative Agreement EAR-0552316. Some activities of are supported by the National Science Foundation EarthScope Program under Cooperative Agreement EAR-0733069. We have used data from the following networks: PS (PACIFIC-21), GE (GEOFON), AU(Geoscience Australia), IU (IRIS/USGS), G (GEOSCOPE), GT (Global Telemetered Seismograph Network -USAF/USGS), YT (POLENET). We thank Masaki Kanao and NIPR (National Institute of Polar Research, Japan) for running SYO station, and providing us with access to recent data through the IFREE (Institute for Research on Earth Evolution) data center at JAMSTEC (Japan Agency for Marine-Earth Science and Technology). The GEOFON network is funded and operated by GFZ Potsdam, Germany, in co-operation with almost 50 institutions worldwide. The IU stations are the part of the Global Seismic Network (GSN) that are installed, maintained and operated by the USGS Albuquerque Seismological Laboratory. Geoscience Australia operates the Australian National Seismic Network within Australia, its Territories and across its local region.

References

- Aster, R.C., D.E. McNamara and P.D. Bromirski (2008), Multidecadal climate-induced variability in microseisms, *Seism. Res. Lett.*, *79(2)*, 194-202, doi:10.1785/gssrl.79.2.194.
- Aster, R.C., D.E. McNamara and P.D. Bromirski (2010), Global trends in extremal microseism intensity, *Geophys. Res. Lett.*, *37*, L14303, doi:10.1029/2010GL043472.
- Barruol, G., D. Reymond, F.R. Fontaine, O. Hyvernaud, V. Maurer and K. Maatuaiahutapu (2006), Characterizing swells in the southern Pacific from seismic and infrasonic noise analyses, *Geophys. J. Int.*, *164*, 516-542, doi:10.1111/j.1365-246X.2006.02871.x.
- Bromirski, P.D., R.E. Flick and N. Graham (1999), Ocean wave height determined from inland seismometer data: Implications for investigating wave climate changes in the NE Pacific, *J. Geophys. Res.*, *104(C9)*, 20,753-20,766, doi: 10.1029/1999JC900156.
- Bromirski, P.D. and F.K. Duennebieer (2002), The near-coastal microseism spectrum: spatial and temporal wave climate relationships, *J. Geophys. Res.*, *107(B8)*, 2166, doi:10.1029/2001JB000265.
- Bromirski, P.D. and P. Gerstoft (2009), Dominant source regions of the Earth's "hum" are coastal, *Geophys. Res. Lett.*, *36*, L13303, doi:10.1029/2009GL038903.
- Cathles, L.M., E.A. Okal and D.R. MacAyeal (2009), Seismic observations of sea swell on the floating Ross Ice Shelf, Antarctica, *J. Geophys. Res. - Earth*, *114*, F02015.
- Cavalieri, D.J., C.L. Parkinson, P. Gloersen and H.J. Zwally (1996, updated 2008), Sea ice concentrations from Nimbus-7 SMMR and DMSP SSM/I passive microwave data, [2000-2009]. Boulder, Colorado USA: National Snow and Ice Data Center. Digital media.

Cavalieri, D.J. and C.L. Parkinson (2008), Antarctic sea ice variability and trends, 1979-2006, *J. Geophys. Res.*, *113*, C07004, doi:10.1029/2007JC004564.

Chave, A.D., D.J. Thomson and M.E. Ander (1987), On the robust estimation of power spectra, coherences and transfer functions, *J. Geophys. Res.*, *92*, 633648.

Chevrot, S., M. Sylvander, S. Benahmed, C. Ponsolles, J.M. Lefevre and D. Paradis (2007), Source locations of secondary microseisms in western Europe: Evidence for both coastal and pelagic sources, *J. Geophys. Res.*, *112*(B11), B11301.

Fetterer, F., K. Knowles, W. Meier and M. Savoie (2002, updated 2009), Sea Ice Index. Boulder, Colorado USA: National Snow and Ice Data Center. Digital media.

Friedrich, A., F. Kruger and K. Klinge (1998), Ocean-generated microseismic noise located with the Graffenberg array, *J. Seismol.*, *2*, 47-64.

Gerstoft, P. and T. Tanimoto (2007), A year of microseisms in southern California, *Geophys. Res. Lett.*, *34*, L20304, doi:10.1029/2007GL31091.

Hasselmann, K. (1963), A statistical analysis of the generation of microseisms, *Rev. Geophys.*, *1*, 177-209, doi:10.1029/RG001i002p00177.

Haubrich, R. and K. Mc Camy (1969), Microseisms: coastal and pelagic sources, *Bull. Seismol. Soc. Am.*, *7*(3), 539-571.

Kedar, E., M. Longuet-Higgins, F. Webb, N. Graham, R. Clayton and C. Jones (2008), The origin of deep ocean microseisms in the North Atlantic ocean, *Proc. R. Soc. A.*, doi:10.1098/rspa.2007.0277.

Longuet-Higgins, M.S. (1950), A theory of the origin of microseisms, *Phil. Trans. Roy. Soc.*, *243*, 1-35.

Stehly, L., M. Campillo and N.M. Shapiro (2006), A study of the seismic noise from its long-range correlation properties, *J. Geophys. Res.*, *111(B10)*, B10306.

Stutzmann, E., G. Roult and L. Astiz (2000), Geoscope station noise level, *Bull. Seismol. Soc. Am.*, *90*, 690-701.

Stutzmann, E., M. Schimmel, G. Patau and A. Maggi (2009), Global climate imprint on seismic noise, *Geochem. Geophys. Geosyst.*, *10*, Q11004, doi:10.1029/2009GC002619.

Tanimoto, T. (2007), Excitation of microseisms, *Geophys. Res. Lett.*, *34*, L05308, doi:10.1029/2006GL029046.

Webb, S.C. (1998), Broadband seismology and noise under the ocean, *Rev. Geophys.*, *36*, 105-142.

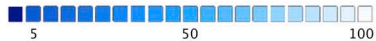
Figure 1. (a) Variations of microseismic power spectral density for station CASY over a 0.1-80 s period band for 2007. Amplitudes are expressed in dB with respect to $1 \text{ m}^2/\text{s}^2/\text{Hz}$, and indicated by the color-bar (gray represents a lack of data). Also shown are ice concentration images from the NSIDC Sea Ice Index [Fetterer *et al.*, 2002] for February, July and December 2007. The approximate location of CASY is indicated by a red triangle. (b) Seismic noise amplitude variations over one year for all Antarctic coastal stations studied. Red triangles represent the locations of the stations. The images near each station show the amplitude variations of seismic noise spectra for different years, chosen for maximum seismic data availability: PMSA 2008, SNAA 2004, SYO 2004, MAW 2008, CASY 2007, VNDA 2006, LONW 2009, SIPL 2009, DRV 2008, SBA 2004.

Figure 2. Seismic noise spectrum variability at SYO over a decade. Annual seismic noise spectra for SYO from 2001 to 2009, using the same color scale as in Figure 1. Also shown are ice concentration images for February and August of each year from the NSIDC Sea Ice Index [Fetterer *et al.*, 2002]. The approximate location of SYO is indicated by a red triangle. Summer microseisms are of lower amplitude during 2005, 2007 and 2008, corresponding to residual ice near the Enderby Land coast (highlighted in magenta).

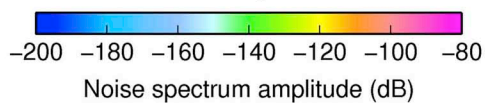
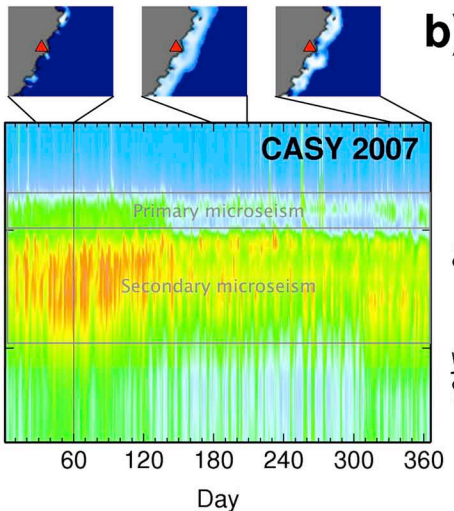
Figure 3. Microseismic spectra over a year for stations SYO and CASY. Each curve represents the seismic noise spectra for one day, color coded by day of the year (see legend). Primary and secondary microseisms are outlined by grey boxes. Summer and winter time peak frequencies are highlighted in red and blue respectively.

Figure 4. Correlation between microseismic noise variations and changes in ice concentrations. (a) Microseismic power at stations SYO (2002), DRV (2005), SBA (2004) and PMSA (2000), using the same color scale as in Figure 1. Years were chosen among those with good seismic data availability. Black and white horizontal lines correspond to periods with strong primary and secondary microseisms respectively. Black vertical arrows on SYO spectrum correspond to anomalous noise signals, and equivalent symbols on PMSA spectrum correspond to absence of primary microseism. (b) Sea-ice concentration from NSIDC [Cavalieri *et al.*, 1996] as a function of distance and time along a 25-km wide beam trending outwards from the coast. Black and white lines and black arrows / symbols correspond to the same time periods as in (a). (c) Red points correspond to the NSIDC grid points that lie along the beams used to create images in (b).

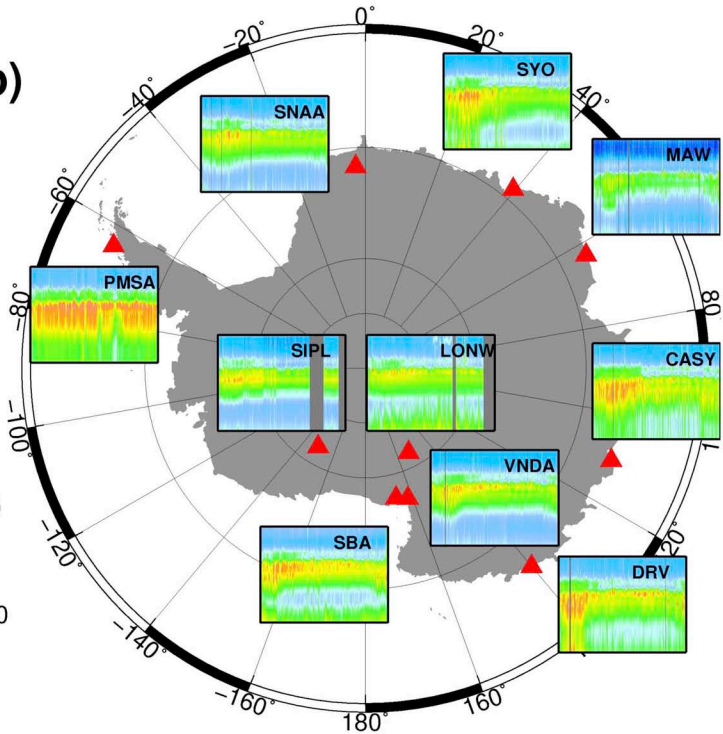
Ice concentration (%)

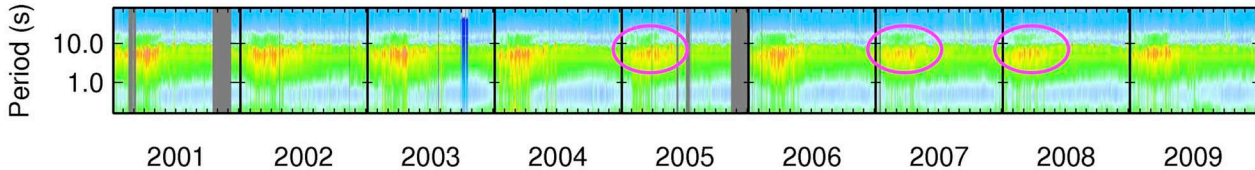


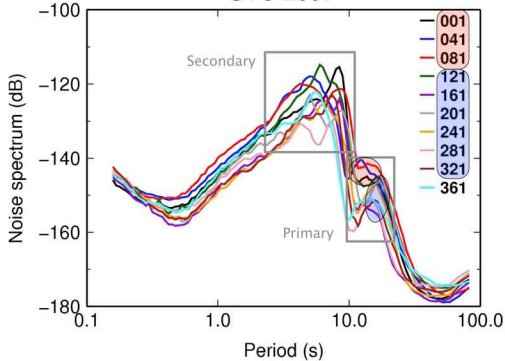
a)



b)





SYO 2007**CASY 2007**